Desalination and Water Treatment
www.deswater.com

doi: 10.5004/dwt.2023.29210

283 (2023) 222–236
January

Adsorption of Crystal violet dye from aqueous solution by activated sewage treatment plant sludge

Priyanka Shrivastava[a], M.K. Dwivedi[a,*], Vibha Malviya[a], Payal Jain[a], Anjali Yadav[a], Neeraj Jain[b]

[a]*Department of Chemistry, Govt. Holkar (Model, Autonomous) Science College, Indore, India, emails: dwivedimk12@gmail.com (M.K. Dwivedi), priyanka191189@gmail.com (P. Shrivastava), vibha220391@gmail.com (V. Malviya), pjain2308@gmail.com (P. Jain), anjaliyadav1899@gmail.com (A. Yadav)*
[b]*CSIR-Central Building Research Institute, Roorkee, India, email: neerajest@rediffmail.com*

Received 2 June 2022; Accepted 9 December 2022

ABSTRACT

Investigations were carried out for the removal of Crystal violet (CV) dye from an aqueous solution using sewage sludge as adsorbent prepared after heating at 900°C. X-ray fluorescence spectroscopy, Fourier-transform infrared spectroscopy, scanning electron microscopy, and X-ray diffraction analysis were used for the characterization of sludge. The results of batch studies showed the values of optimum parameters such as contact time (180 min), adsorbent dose 10 g/L and temperature (30°C). The removal efficiency was found to be about 98.4% and the equilibrium adsorption capacity of Crystal violet dye was 9.508 mg/g. The Freundlich, Langmuir, Redlich–Peterson, and Dubinin–Radushkevich isotherms were employed to evaluate the equilibrium data from batch adsorption studies. Kinetic data were analyzed using kinetic models such as; pseudo-first-order, pseudo-second-order, intraparticle diffusion. Nonlinear regression method and error functions namely; R^2, sum of error squares, G^2, HYBRID, Marquardt's percent standard deviation, root mean square error and mean square error were used to determine the best fitted model. Freundlich isotherm model best fitted the data showing multilayer adsorption of CV dye on activated sludge while kinetic studies of CV dye were well described by pseudo-second-order model. Thermodynamic characteristics for dye adsorbent system indicated that the adsorption process was spontaneous and endothermic in nature. Results show that activated sludge can be effectively used as low-cost adsorbent for the removal of cationic dyes from aqueous solution.

Keywords: Adsorption; Crystal violet; Sewage sludge; Thermodynamic studies; Error function

1. Introduction

The key factor influencing a country's economic development and the development of society is industrialization. Both in developing and developed nations, several large and medium-sized industries are crucial to a country's economic development [1]. The textile industry occupied the greater part because of its ability to generate a wide range of employment possibilities and its connection with many local and international economic sectors. The major raw materials used throughout in these industries are cotton, wool, synthetic fibres, synthetic dyes, chemicals, and process water. All of these materials diversify the textile industry's economic significance. Toxic contaminants such as dyes, NaOH, starch, acid, etc. are present in the wastewater discharged by the textile industry [2]. Water pollution is a major issue throughout the world due to rapid industrialization. It is due to the accumulation of physical

---

* Corresponding author.

and chemical substances from natural or manmade sources [3]. In comparison to other industries, textile industries are estimated to use more potable water and chemicals, and nearly all of their effluents are heavily polluted. On average, the textile sector uses 200 L of potable water every kilogram of product [4]. According to Bhatt and Rani [5], the World Bank estimates that the dyeing and finishing sector generates approximately 17%–20% of all industrial effluent. Therefore, wastewater treatment plays an important role in developing strategies for the management of water resources [6].

The discharge of dye containing effluent into the wastewater is harmful because of their chemical composition and toxicity [7–9]. Dyes are complicated molecules that are very difficult to degrade naturally in the water system [10]. One of the severe environmental issues about dyes is that they reduce light penetration into the water, which has negative impacts on aquatic life and results in oxygen deficiency [11,12].

Crystal violet (CV) dye is mainly used in textile, printing ink and dyeing, leather manufacturing, food industries, veterinary medicine, and drugs [13,14]. It also has antibacterial and antifungal properties [15]. The wastewater generated by Crystal violet has a dark purple color, high concentration as well as poor biodegradability. Crystal violet dye is carcinogenic, mutagenic, and teratogenic, which has very harmful effects on human beings as well as aquatic life [16]. It may cause eye burns leading to the permanent cornea or eye damage [17]. It leads to respiratory failure, brain confusion, and studies indicated that the accumulation of Crystal violet dye has been suspected to cause cancer in human beings [18]. Therefore, an effective technique for the treatment of Crystal violet dye is needed to prevent further contamination of surface water. Various conventional methods such as, ion-exchange, coagulation–flocculation [19], membrane separation, biological degradation, and adsorption are utilized for the dye removal [20–28]. The adsorption method has advantages over other technology because of simplicity of design, low cost and prevention of dangerous chemicals generated during the process [29]. Due to high cost involved in preparation of commercially available adsorbents, researchers are focusing on utilization of low-cost adsorbents. Recently low-cost adsorbents have been used to adsorb dyes from wastewater [30–36]. For the treatment of organic substances in wastewater, advanced oxidation techniques including ozonation, Fenton processes, photocatalysis, and electro-oxidative have been used. They are extremely reactive, non-selective, and effective for reducing organic substances from wastewater with the help of hydroxyl radicals produced by advanced oxidation technology. Ozone-based processes do have some drawbacks, such as the high cost of O_3, low water solubility, and the occurrence of some dangerous by-products. Advanced oxidation processes may occasionally be suppressed by the use of strong radical scavenging agents from wastewater. Fenton-based methods have the potential to produce undesired iron sludge and necessitate pH settings that are impractical [37–39].

Conventional wastewater treatment technologies are not much effective for dye removal in pulp and paper industry. Hence, a novel Fe-zeolite catalyst was developed for the catalytic ozonation process [40]. The mechanism of the catalytic ozonation process was explained by studying the production of reactive oxygen species, such as hydroxyl radicals, superoxide ion radicals, and hydrogen peroxide [41]. Catalytic ozone removal efficiency of erythromycin was studied in simple ozonation and catalytic ozonation using iron-loaded rice husk ash and peanut shell ash [42].

Some economic and effective adsorbents have been used for the removal of Crystal violet dye, such as aerogel prepared by chitin-psyllium [43], cocoa pod powder [44], carbon composite [45], olive leaves powder [46], coniferous pinus bark [47], rice husk [48], date palm fiber [49], chitosan composite [50], modified fly ash [51], coconut husk powder [52], bottom ash [53], grapefruit peel [54] and pea peels [55]. Recently PBC (plant biomass carbon) is also used as economic adsorbent for the removal of dyes [56].

Sludge generated from sewage treatment plants (STP) normally is in the form of semi-solid waste or slurry. It has to go through further treatment before being suitable for disposal. Currently, around 62.5% of undigested sewage sludge is being generated in India [57], hence the safe disposal of sewage sludge is important for the protection of human health and environment [58–61]. Sludge is being utilized in the cement industry as an alternative fuel source and is frequently disposed off on agricultural lands for manure purposes [62]. Sewage sludge has been used successfully in the removal of dyes from wastewater [63–65]. However, very little work is reported for the use of activated STP sludge as an adsorbent for the removal of cationic dyes from wastewater [66–68].

In present studies, activated STP sludge was used as adsorbent to investigate equilibrium, kinetic, and thermodynamic studies for the removal of Crystal violet dye from aqueous solution.

2. Experimental

2.1. Materials and methods

"Cationic Crystal violet ($C_{25}H_{30}N_3Cl$; N-[4-[bis[4-dimethylamino)-phenyl]-methylene]-2,5-cyclohexadien-1-ylidine]-N-methylmethanaminium chloride; molecular mass = 407.98 g/mol;) also known as Basic Violet 3, Gentian Violet, and Methyl Violet 10B was supplied by Merck, India. For the preparation of stock solution, Crystal violet (1.0 g) was dissolved in 1.0 L of distilled water. The test solution of desired concentrations was obtained by diluting the stock solution with reasonable volume of distilled water. Analytical grade reagents were used in the study. All the experiments were performed in duplicate and only the mean values are reported. The maximum deviation was found to be less than ±4%.

2.2. Adsorbent development

Sludge sample was collected from the sewage treatment plant (STP) Okhla, New Delhi, India. Sewage sludge was activated in the furnace at 900°C for 30 min. Conditions of activation had been carefully managed to get the product having batch-to-batch reproducibility. The developed adsorbent was sieved to 100–150 μm particle size. Table 1 shows the physiochemical properties of STP sludge.

Table 1
Physical properties of As collected sewage sludge

Properties	Values
pH	6.80
Colour	Light brown
Specific gravity	1.91
Bulk density	2.42 g/cm^3
BET surface area	25.84 m^2/g
LOI	40.20
Fineness modulus	1.09

2.3. Adsorption studies

Sorption studies of Crystal violet dye were performed to obtain rate and equilibrium data in aqueous suspensions using activated sewage sludge as adsorbent. A series of 50 mL beaker were used for these experiments. Each beaker was filled with 20 mL of dye solution of varying concentrations and the pH and temperature were adjusted to the correct levels. Each beaker was stirred at 100 rpm after a known amount of adsorbent was applied. The sample was shaken in a temperature controlled shaking machine for maximum period of 3 h. The equilibrium time of 3 h was found to be sufficient for maximum uptake. After this period the supernatant solution was centrifuged and piped separately before being evaluated with a spectrophotometer (CHEMI LINE Digital Spectro Photometer CL-320) by measuring the absorbance at 580 nm. The concentration of dye was calculated by taking the difference in initial and final concentration. Initial dye concentrations taken for experimentation were 2–50 mg/L The selected concentration range was ascertained after a good deal of preliminary examination.

After establishing the equilibrium, the dye solution was centrifuged. The difference between the initial and final Crystal violet dye concentrations was used to calculate the amount of dye adsorbed at time t, q_e (mg/g), as illustrated in the equation:

$$q_e = \frac{\left(C_0 - C_e\right)V}{W} \tag{1}$$

where q_e (mg/g) is the amount of dyes adsorbed, and C_o (mg/L) is the initial dye concentration, while C_e (mg/L) is the concentration of dye in solution at equilibrium, V (L) is the volume, and W (g) is the weight of adsorbent.

The percentage removal of the dye was computed using the following equation:

$$\%\text{Removal} = \frac{\left(C_0 - C_e\right)}{C_0} \times 100 \tag{2}$$

where C_o is the initial concentration and C_e is the equilibrium concentration of Crystal violet dye (mg/L).

2.4. Adsorption isotherms

The adsorption mechanism, surface characteristics, and affinity of the adsorbent are frequently shown via adsorption equilibrium models. Freundlich, Langmuir, Redlich–Peterson, and Dubinin–Radushkevich isotherms are the most widely employed equilibrium models.

Freundlich isotherm model proposed by Freundlich (1906) is based on the assumption that the adsorption occurs onto a heterogeneous surface [69]. Because of the differences in interactions between the adsorbed molecules, the sites with the maximum affinity are filled first, resulting in multilayer adsorbate molecule formation. The nonlinear expression of the Freundlich isotherm is written as Eq. (3):

$$q_e = K_f C_e^{\frac{1}{n}} \tag{3}$$

where K_f is the constant indicating the adsorbent's relative adsorption capacity (m/g), and $1/n$ is the constant indicating the adsorption intensity. K_f and $1/n$ are two constants in the Freundlich equation. The magnitude of $1/n$ ranges between 0 and 1, which showed favorable adsorption.

The Langmuir isotherm assumes that maximal adsorption corresponds to a saturated monolayer of solution on a homogeneous adsorbent surface. It is made up of a finite number of identical sites that have the same adsorption energy. Adsorption occurs within the adsorbent at certain homogenous sites. Once a molecule occupied a site, no more transmigration can occur at the same site. The adsorbent's total monolayer capacity is equal to a Langmuir constant (q_m). The equation was developed by Irving Langmuir in 1916 [70]. The Langmuir isotherm model in its nonlinear form is expressed as Eq. (4).

$$q_e = \frac{K_L q_m C_e}{1 + K_L C_e} \tag{4}$$

where C_e is the dye equilibrium concentration (mg/L), q_e is the quantity of dye adsorbed at equilibrium (mg/g), q_m is the monolayer adsorption capacity (mg/g), and K_L is the constant associated to the free energy of adsorption.

Redlich–Peterson isotherm (Redlich and Peterson 1906) is a combination of Langmuir and Freundlich isotherms [71]. This model is defined by the following expression:

$$q_e = \frac{AC_e}{1 + BC_e^g} \tag{5}$$

where A is the Redlich–Peterson isotherm constant (L/mg), B is the constant (L/mg), g is an exponent ranging from 0 to 1, C_e is the equilibrium liquid-phase concentration of the adsorbent (mg/L), and q_e is the equilibrium adsorbate loading on the adsorbent (mg/g).

The Dubinin–Radushkevich isotherm is commonly used to characterize the adsorption mechanism onto a heterogeneous surface with a Gaussian energy distribution [72]. The Dubinin–Radushkevich isotherm's nonlinear form is defined as:

$$q_e = q_D \exp\left[-K_D \left\{\ln\left(1 + \frac{1}{C_e}\right)^2\right\}\right] \tag{6}$$

where q_D (mg/g) is the Dubinin–Radushkevich isotherm constant and K_D (mg/g) is the activity coefficient ($K_D = \beta_D R^2 T^2$). The values of adsorption energy (E) at the different temperature were calculated using Eq. (7).

$$E = \frac{1}{\sqrt{2\beta_D}} \tag{7}$$

2.5. Kinetic studies

One of the most essential parameters in determining adsorption efficiency is adsorption kinetics. The kinetic data was analyzed using four well-known kinetic models: pseudo-first-order, pseudo-second-order, intraparticle diffusion, and Elovich model.

Kinetic tests were carried out in batches at 30°C and pH 5.0 with a fixed dose of adsorbent (10 g/L) and 5, 10 and 20 mg/L of initial dye concentrations. The adsorbent was separated by filtering at a certain time interval, and the filtrate was measured on a spectrophotometer to determine the dye's equilibrium concentration. The rate of solute uptake at the solid-solution interface is described by adsorption kinetics.

The pseudo-first-order kinetic model proposed by Lagergren (1898), was used to investigate the rate constant of dye adsorption onto sewage sludge [73]. The nonlinear form of the pseudo-first-order model is given as in Eq. (8):

$$q_t = q_e\left(1 - e^{-K_{\mathrm{ad}}t}\right) \tag{8}$$

where q_e is the amount of dye adsorbed at equilibrium, and q_t is the amount of dye adsorbed at time t (both in mg/g).

The pseudo-second-order kinetic model (Ho and McKay [74]) assumes a second-rate kinetic mechanism for adsorption. Chemisorption, which involves the sharing or exchange of electrons between the solute and the sorbent, is described in the model as controlling the sorption process. Pseudo-second-order kinetic in its nonlinear form is expressed as Eq. (9):

$$q_t = \frac{K_2 q_e^2 t}{1 + K_2 q_e t} \tag{9}$$

where q_e represents the amount of adsorption at equilibrium (mg/g), q_t represents the amount of adsorption at time t (mg/g), and K_2 represents the pseudo-second-order rate constant (g/mg·min).

Intraparticle diffusion is the rate limiting during the second-step of the adsorption cycle and it slows down in the third step due to the presence of less amount of adsorbate into the solution. The experimental data was fitted to the Weber–Morris equation, which informed that the adsorption capacity varies almost proportionally to $t^{0.5}$ and expressed as Eq. (10):

$$q_t = K_{\mathrm{int}} t^{0.5} + C_i \tag{10}$$

where q_t is the adsorption capacity at time (t), K_{int} (mg/g·min$^{0.5}$) is the intraparticle diffusion rate constant and C_i is the intercept. The intraparticle diffusion mechanism was not solely controlling adsorption kinetics as the plot did not pass through the origin [75,76]. Elovich model (Ho and McKay [77]) is based on multilayer adsorption and adsorption increases exponentially with the adsorption site. The nonlinear form of Elovich kinetics model is given by Eq. (11):

$$q_t = \frac{1}{\beta}\ln\left(1 + \alpha\beta t\right) \tag{11}$$

where the initial adsorption rate (mg/g min) is known as α, and the parameter β is related to the extent of surface covering and chemisorption activation energy (g/mg).

2.6. Thermodynamic studies

The thermodynamic characteristics of the adsorption experiments were analyzed using the following equations:

$$\log\left(\frac{q_e}{C_e}\right) = \frac{\Delta S^\circ}{2.303R} - \frac{\Delta H^\circ}{2.303RT} \tag{12}$$

$$\Delta G^\circ = \Delta H^\circ - T\Delta S^\circ \tag{13}$$

where ΔG°, ΔH° and ΔS° denote the changes in free energy, enthalpy, and entropy, respectively, whereas R (8.314 J/mol·K) and T (K) have their usual connotations.

2.7. Nonlinear regression analysis

The conventional way of determining the isotherm parameters using the linearized models has a major disadvantage because the inherent bias resulting from linearization may cause the R^2 not able to provide the best isotherm constants to correlate with the original isotherm [78]. The most popular method for obtaining the isotherm parameters as linear regression using the least-squares method. The error functions that created the least error distribution between the predicted and experimental isotherms were used to choose the best-fit isotherm. It involves entering first the experimental data, equilibrium concentration (C_e) and amount of dye adsorbed at equilibrium (q_e for sorption equilibrium, q_t for sorption kinetics) into the Excel Spreadsheet and graphing the data. The nonlinear regression analysis is conveniently carried out using the Solver add-in function in the Microsoft Excel spreadsheet.

2.8. Error function analysis

Different error parameters were calculated to identify the most suitable isotherm and kinetic models that describe the treatment process. The nonlinear form was a good alternative parameter that provided an accurate technique to determine isotherm and kinetic parameters from the original equation forms [79–82]. The error function is required to evaluate the best fit of nonlinear models [83]. Error functions are statistical equations that are used to calculate the difference between theoretically expected data and actual experimental data values. Seven alternative statistical error functions used to validate the best-fitting sorption kinetic and equilibrium isotherm models are: coefficient of determination (R^2), chi-square (χ^2), sum of error squares (SSE), log-likelihood test (G^2), hybrid fractional error function (HYBRID), Marquardt's percent standard deviation (MPSD), root mean square error (RMSE) and mean square error (MSE) (Table 2) [84–91]. The best-fit model is the one with the lowest error function value and highest R^2 value.

3. Results and discussion

Sewage sludge sample collected from sewage treatment plants were characterized using X-ray fluorescence spectroscopy (XRF), Fourier-transform infrared spectroscopy (FTIR), scanning electron microscopy (SEM), and X-ray diffraction (XRD) analysis.

3.1. Chacterization

3.1.1. Energy-dispersive X-ray spectroscopy analysis

EDAX stands for energy-dispersive X-ray spectroscopy, which is an analytical technique used to identify the elemental composition of materials (Table 3). EDAX spectra of As collected sewage sludge are shown in Fig. 1. XRF analysis is the latest technique for the identification of elements present in the sample but it cannot provide information regarding low atomic number elements (less than 16).

3.1.2. X-ray fluorescence analysis

XRF spectrometer VEXTA (Pk596-B) model was used for the determination of elemental composition of sludge sample using X-ray fluorescence analysis (Fig. 2). Table 4 shows the elements found in sewage sludge samples. Two major elements Fe and Ca, eight minor elements (Sr, K, Zn, Zr, Ti, S, Rb, Cu), and four trace elements (Y, As, Br, Cl) below 0.5% in STP sludge were observed [92]. The concentration of majority of elements increased after the activation of sewage

Table 3
EDAX analysis of As collected sewage sludge

Element	App	Intensity	Weight %	Weight %	Atomic %
	Conc.	Corrn.		Sigma	
O K	39.11	0.6050	51.00	1.30	70.87
Mg K	2.05	0.6866	2.36	0.38	2.16
Si K	15.08	0.7392	16.10	0.74	12.75
P K	4.61	0.9292	3.91	0.49	2.81
S K	0.74	0.7295	0.80	0.27	0.56
K K	1.49	0.9979	1.17	0.32	0.67
Ca K	12.92	0.9561	10.67	0.65	5.92
Fe K	3.44	0.8375	3.24	0.72	1.29
Br L	9.88	0.7264	10.74	0.81	2.99
Total			100.00		

Table 2
Different error functions used for the equilibrium isotherms and kinetics analysis

Error functions	Abbreviation	Expression	References
Coefficient of determination	R^2	$\sum_{i=1}^{n}\frac{\left(q_{e,\exp}-q_{e,\mathrm{cal}}\right)^2}{\left(q_{e,\exp}-q_{e,\mathrm{mean}}\right)^2}$	[84]
Chi-square	$\chi2$	$\sum_{i=1}^{n}\frac{\left(q_{e,\exp}-q_{e,\mathrm{cal}}\right)^2}{q_{e,\mathrm{cal}}}$	[85]
Sum of error squares	SSE	$\sum_{i=1}^{n}\left(q_{e,\exp}-q_{e,\mathrm{cal}}\right)^2$	[86]
Log-likelihood test	G^2	$2\sum_{i=1}^{n}\left(q -_{e,\exp}\times\ln\left(\frac{q_{e,\exp}}{q_{e,\mathrm{cal}}}\right)\right)$	[87]
Hybrid fractional error function	HYBRID	$\frac{100}{n}\sum_{i=1}^{n}\frac{\left(q_{e,\exp}-q_{e,\mathrm{cal}}\right)^2}{q_{e,\exp}}$	[88]
Marquardt's percent standard deviation	MPSD	$100\sqrt{\frac{1}{\left(n-p\right)}\sum_{i=1}^{n}\left(\frac{q_{e,\exp}-q_{e,\mathrm{cal}}}{q_{e,\exp}}\right)^2}$	[89]
Root mean square error	RMSE	$\sqrt{\sum_{i=1}^{n}\frac{\left(q_{e,\exp}-q_{e,\mathrm{cal}}\right)^2}{n}}$	[90]
Mean square error	MSE	$\frac{1}{n}\sum_{i=1}^{n}\left(q_{e,\exp}-q_{e,\mathrm{cal}}\right)^2$	[91]

sludge and decreased after dye adsorption. Heavy metals such as zinc, copper and arsenic were detected in sewage sludge but their concentrations were found to be within the permissible limit of WHO as prescribed by EPA [93].

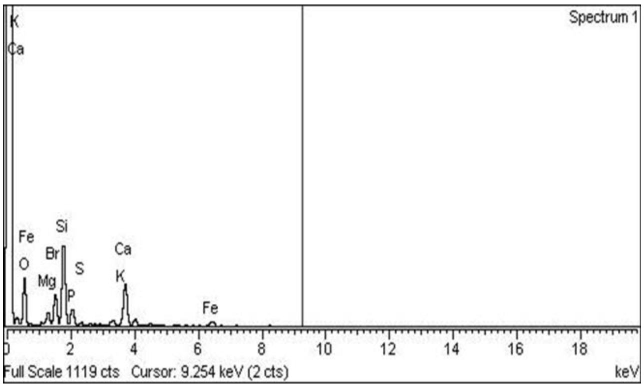

Fig. 1. EDAX spectra of As collected sewage sludge.

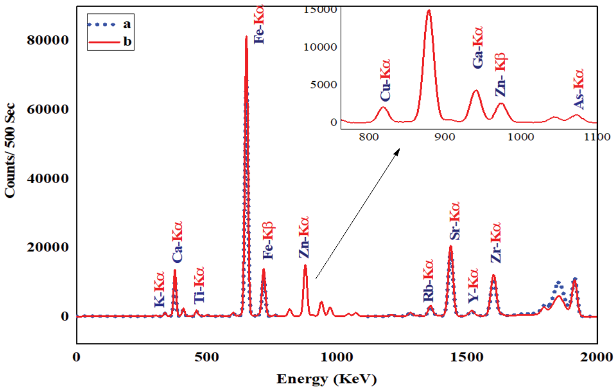

Fig. 2. XRF spectra of (a) As collected sewage sludge and (b) activated sewage sludge samples.

Table 4
Elemental composition of sewage sludge samples

Elements	As collected sewage sludge wt.%	Activated sewage sludge wt.%
Fe	0.45	0.82
Ca	0.40	0.81
K	0.06	0.11
Sr	0.06	0.09
Zn	0.05	0.08
S	0.04	0.02
Zr	0.04	0.07
Ar	0.03	0.05
Ti	0.03	0.05
Cl	0.01	–
Rb	0.01	0.01
Mn	0.01	0.01
Cu	0.01	0.01

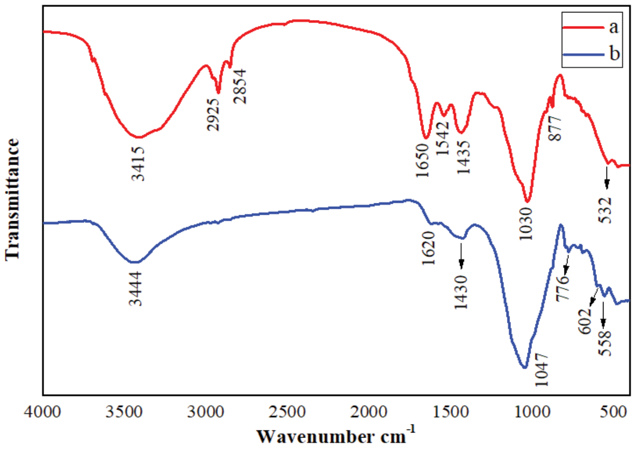

Fig. 3. FTIR analysis spectra of (a) As collected sewage sludge and (b) activated sewage sludge samples.

3.1.3. FTIR analysis

FTIR spectra were obtained using a Bruker Vertex 80V spectrometer (4,000–400 cm^{-1}) (Fig. 3). The presence of alcohols in As collected sewage sludge was detected due to hydroxyl group (O–H) stretching vibrations at 3,415 cm^{-1}. This band shifted to 3,444 cm^{-1} in activated sludge and 3,420 cm^{-1} in Crystal violet dye treated sewage sludge. The peak's broadening could be related to the activation of sewage sludge at high temperatures. The existence of the –COOH group was detected by the O–C=O linkage at 1,435–1,430 cm^{-1} in collected and activated sewage sludge, however this band shifted to 1,450 cm^{-1} in dye-treated sewage sludge. Asymmetric C–H stretching vibrations could be responsible for the absorption band about 2,925 cm^{-1} (weak peak). The bands that appeared at 1,620–1,650 cm^{-1} represented the aromatic ring's C=C stretching vibration. A distinctive peak for C–X halogen stretching vibration were found at 1,030 and 1,047 cm^{-1} for As collected and activated sewage sludge samples, respectively. Various bands connected to aromatic, out-of-plane C–H bending with varying degrees of substitution were found in the 600–900 cm^{-1} range [94,95].

3.1.4. SEM analysis

The particle morphology and surface structure of sewage sludge were investigated using SEM analysis (Fig. 4). The majority of the particles in the sewage sludge were of various sizes and shapes, resulting in an increase in the adsorbent pore volume. The accumulation of particles on the surface of sewage sludge caused the surface to become rough. SEM analysis was performed at RRCAT Indore, India, using 1GMA, the ZEISS Gemini instrument

3.1.5. XRD analysis

The XRD pattern (Fig. 5) confirmed the presence of SiO_2, $CaCO_3$, $ZnSO_4$, Fe_3O_4, SrO_2, ZrO_2, FeO and SrO_2 phases in As collected and activated sewage samples and their concentrations are shown in Table 5.

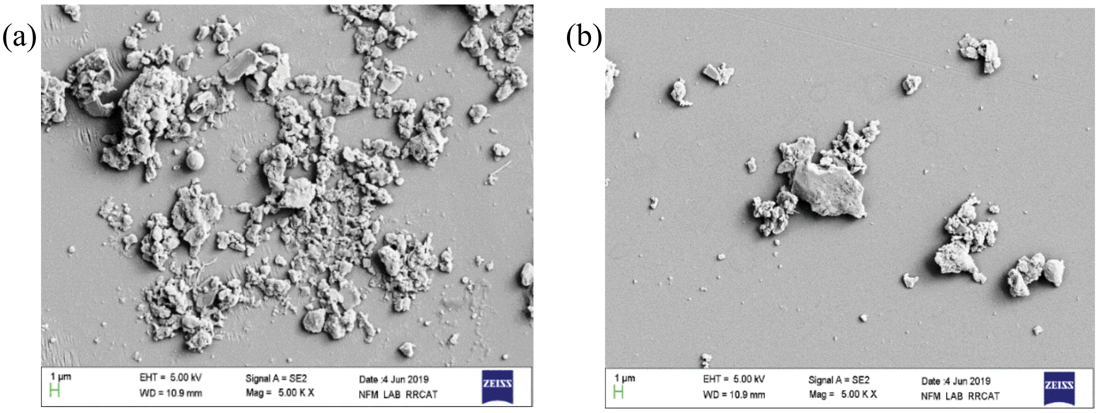

Fig. 4. SEM analysis of (a) As collected and (b) activated sewage sludge samples.

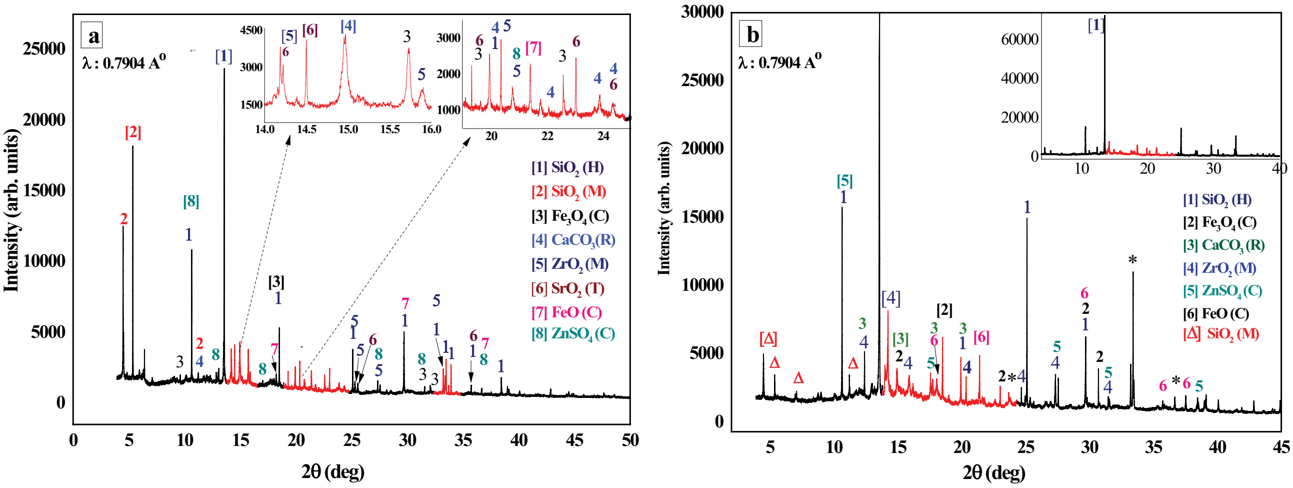

Fig. 5. XRD analysis of (a) As collected and (b) activated sewage sludge samples.

Table 5
XRD analysis of sewage sludge samples

Chemical formula	As collected sewage sludge wt.% (±0.2)	Activated sewage sludge wt.% (±0.2)
SiO_2 (M)	47.3	4.0
SiO_2 (H)	26.6	64.1
$CaCO_3$ (R)	6.3	5.1
$ZnSO_4$ (C)	6.9	9.7
Fe_3O_4 (C)	8.6	10.2
SrO_2 (T)	2.3	–
ZrO_2 (M)	1.0	5.6
FeO (C)	1.0	1.2

3.2. Adsorption studies

3.2.1. Effect of contact time

The effect of contact time on Crystal violet dye adsorption was investigated at two different concentrations (5 and 10 mg/L) with a fixed adsorbent dosage of 5 g/L at 30°C over different time intervals (15–240 min). Fig. 6a shows that the maximum adsorption occurred within the first 180 min, after that no noticeable change was observed. As a result, 180 min was determined to be an optimum contact time for the removal of Crystal violet dye. According to the experimental data, the maximum adsorption was found to be 98.08% and 86.97% at 10 and 5 mg/L, respectively. Same contact time have also been reported in experimental modelling studies on the removal of Crystal violet, methylene blue and malachite green dyes using Theobroma cacao (cocoa pod powder) [44] and adsorption of hazardous Crystal violet dye by almond shells and determination of optimum process conditions by Taguchi method [96].

3.2.2. Effect of pH

As described in Fig. 6b, the influence of pH was investigated at different pH values ranging from 4.0 to 10.0. The experiments were conducted at two concentrations (5 and 10 mg/L), with a 5 g/L adsorbent dosage, at 180-min of contact time and a temperature of 30°C. The pH was changed by adding 0.1 M HCl or 0.1 M NaOH. It was found that on increasing the pH 4.0 to pH 5.0 the sorption capacity of Crystal violet dye increased. After pH 5.0, the adsorption decreased due to precipitation. At an optimal pH of 5.0, removal of Crystal violet dye was found to be 88.04% (5 mg/L) and 95.91% (10 mg/L), respectively. This variation is quite similar to the work done by Sultana et al. [52].

Zero-point charge (ZPC) of the sewage sludge was found to be 3.5 which is quite similar to the study reported in literature [97]. When pH > pHzpc, the adsorbent has negative surface charges and the adsorption of cations are favored. According to the obtained results, by increasing the pH from 4.0 to 5.0, the Crystal violet dye adsorption efficiency increased. This can be due to the strong gravitational force and the reduction of repulsive force between the adsorbent surface and the Crystal violet dye [54]. As pH increased, increase in surface charge density of adsorbent results in decrease of adsorption due to electrostatic repulsion [49].

3.2.3. *Effect of adsorbent dose*

A series of adsorption experiments were carried out with different adsorbent dosages ranging from 5 to 25 g/L at an initial dye concentration of 5 and 10 mg/L at pH 5.0 and temperature 30°C to study the influence of adsorbent dose on the adsorption of Crystal violet dye. The contact time was maintained at 180 min, and the results are reported in Fig 7a. The percentage removal efficiency of Crystal violet dye first increased with an increase in adsorbent dosage from 5 to 10 g/L, but thereafter decreased. The maximum adsorption found to be 90.16% and 98.33% for dye concentrations of 5 and 10 mg/L, respectively at adsorbent dose of 10 g/L. The increase in adsorption with adsorbent dosage can be attributed to an increase in the adsorption surface and availability of more adsorption sites [98]. Similar findings were reported in the adsorption of Crystal violet dye by Laskar and Kumar [99].

3.2.4. *Effect of initial adsorbate concentration and temperature*

The effect of initial concentration of Crystal violet dye in the range of 2–50 mg/L was carried out to observe the adsorption efficiency of activated sludge at a fixed adsorbent dosage (10 g/L) and temperatures (30°C, 40°C and 50°C). The pH was maintained at 5.0 and contact time was kept 180 min. The results of the studies are shown in Fig. 7b which showed that dye uptake increased with an increase

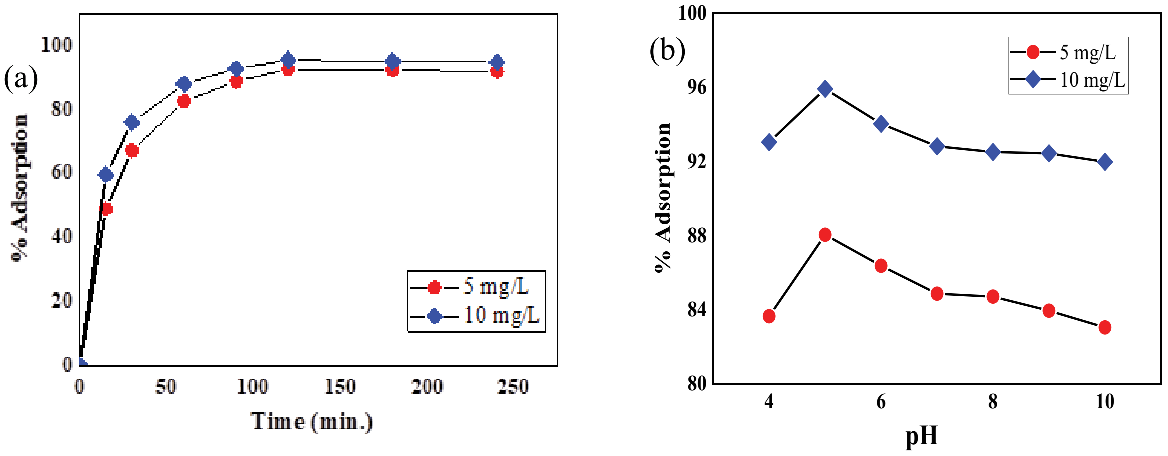

Fig. 6. Effect of (a) contact time and (b) effect of pH on Crystal violet dye adsorption.

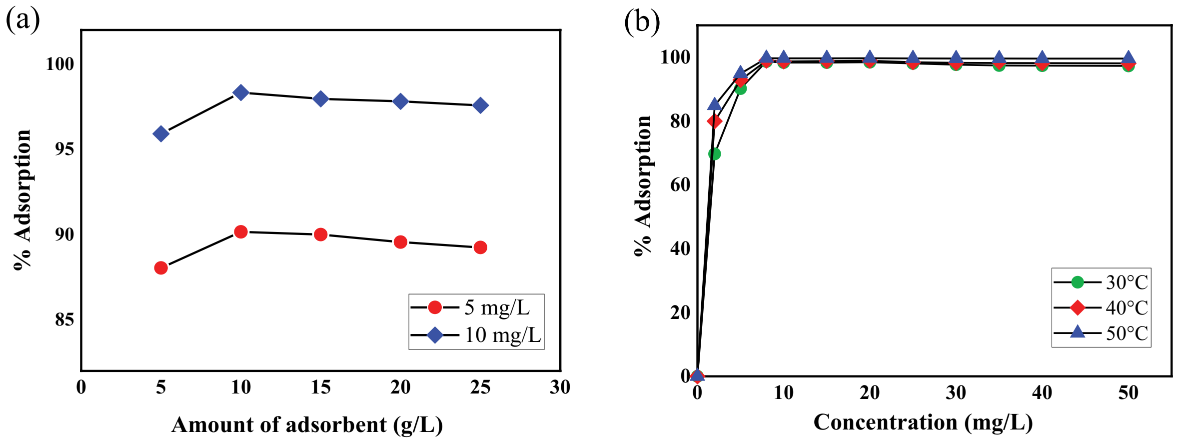

Fig. 7. Effect of (a) adsorbent dose and (b) initial adsorbate concentration and temperature on Crystal violet dye adsorption.

in initial Crystal violet concentration from 2–20 mg/L and thereafter equilibrium was achieved in dye uptake efficiency. The increment in sorption capacity might be due to the increase of dye concentration which resulted in a higher concentration gradient of the dye, thus leading to higher sorption capacity. The rate of uptake of dye slightly increased with increase in temperature thereby indicating the process to be endothermic. The similar result was reported in adsorption of Crystal violet dye from wastewater by waste materials [53].

3.3. Adsorption isotherms

Non-linear analysis and error function analysis for the isotherms of the sorption of Crystal violet dye was calculated with the help of Solver add-in function in Microsoft Excel. Predicted curve for the various adsorption isotherms such as Freundlich, Langmuir, Redlich and Dubinin were fitted for Crystal violet dye at 30°C, 40°C and 50°C (Figs. 8a–c). Results are summarized in Table 6. It was found that Freundlich model fitted well with a higher correlation coefficient (R^2 = 0.9866) as compared to Langmuir (R^2 = 0.9810), Redlich–Peterson (R^2 = 0.9280) and Dubinin–Radushkevich (R^2 = 0.9421), It showed that distribution of active sites of the adsorbent was exponential, and the adsorption process occurred on a heterogeneous surface of the adsorbent. The value of n (1.4178) was found between 1 and 10 which showed the favorable adsorption of CV on the activated sewage sludge (Wong et al. [78]). In addition, the lowest value of χ^2 (0.0761) confirmed the fitness of Freundlich isotherm model.

The adsorption capacity of various low-cost adsorbent used previously for the adsorption of Crystal violet dye are mentioned in Table 7 [100–106] which shows that the activated sludge has better adsorption capacity as compared to most of the other low-cost adsorbents.

3.4. Kinetic studies

Predicted curves for the pseudo-first-order, pseudo-second-order, intra particle diffusion and Elovich kinetic models were fitted for Crystal violet dye onto activated sewage sludge at different concentrations (5, 10 and 20 mg/L) and different temperatures: viz. 30°C, 40°C and 50°C as shown in Figs. 9a–e. Error function analysis for kinetics of the sorption of Crystal violet dye were calculated with the help of Solver add-in function in Microsoft Excel. Results are summarized in Table 8.

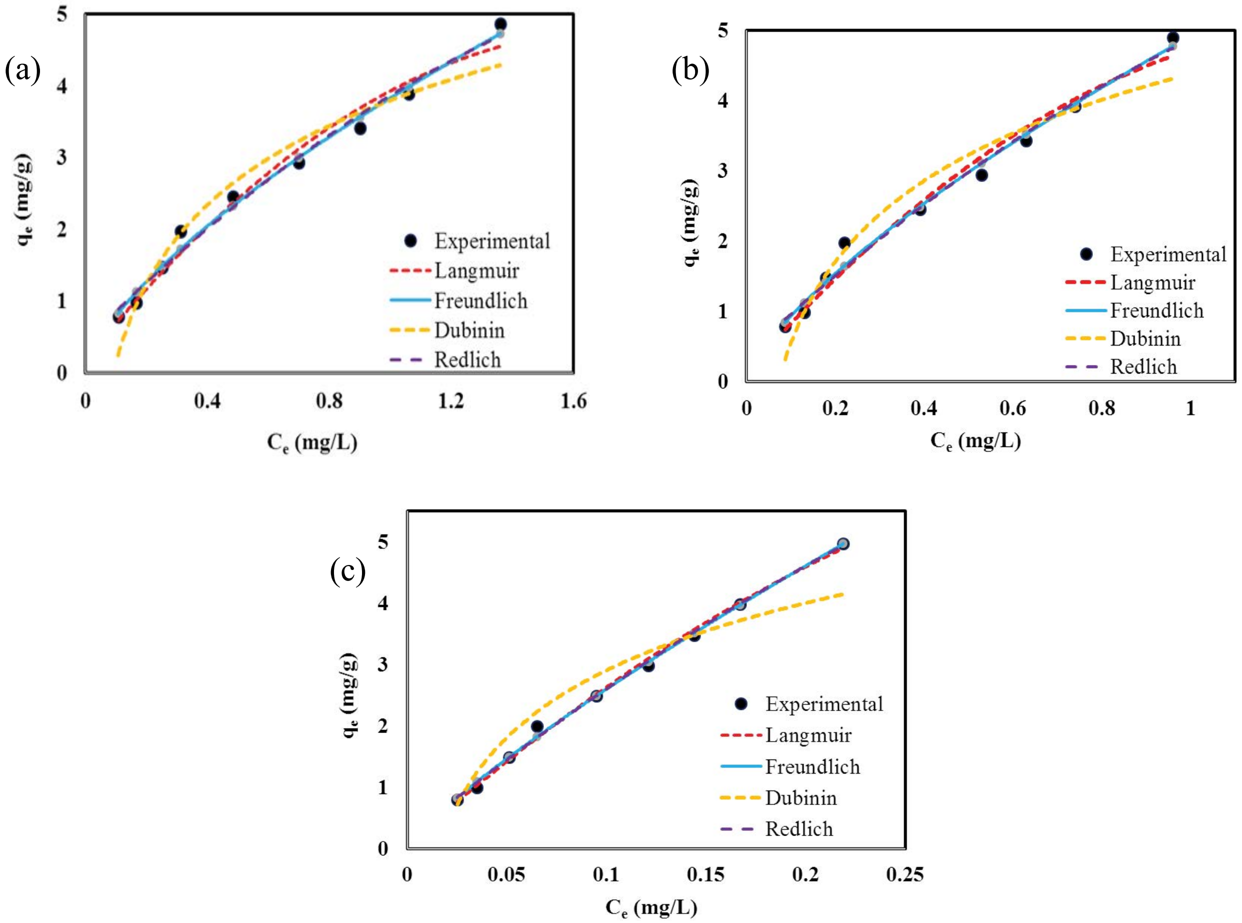

Fig. 8. Predicted curve fits for the equilibrium isotherms of Crystal violet dye sorption onto sewage sludge at (a) 30°C, (b) 40°C and (c) 50°C.

Table 6
Parameters and error function data for adsorption isotherm models of Crystal violet dye onto activated sewage sludge

Isotherm model	Parameters	30°C	40°C	50°C
Freundlich	K_f (mg/g)	3.8304	4.9226	17.418
	n	1.4628	1.3832	1.2107
	R^2	0.9898	0.9877	0.9972
	χ^2	0.0761	0.1046	0.0272
	SSE	0.1540	0.1881	0.0439
	G^2	0.0523	0.1256	–0.0131
	HYBRID	1.0630	1.3773	0.3820
	MPSD	8.0879	9.1506	5.1890
	RMSE	0.1308	1.4456	0.0699
	MSE	0.0171	0.0209	0.0049
Langmuir	$Q_{\max}$ (mg/g)	9.1335	10.641	17.447
	K_L	0.7403	0.8120	1.7827
	R^2	0.9817	0.9789	0.9960
	χ^2	0.1126	0.1536	0.0309
	SSE	0.2762	0.3254	0.0637
	G^2	0.4682	0.5774	0.1924
	HYBRID	1.5016	1.9636	0.4168
	MPSD	8.9339	9.9901	4.7982
	RMSE	0.1751	0.1902	0.0841
	MSE	0.0306	0.0362	0.0071
Redlich–Peterson	A (L/g)	110.60	151.02	58.713
	B (mg/g)$^{-g}$	27.866	29.730	2.5630
	g	0.3305	0.2899	0.3120
	R^2	0.9898	0.9877	0.9973
	χ^2	0.0769	0.1043	0.0247
	SSE	0.1540	0.1888	0.0427
	G^2	0.0555	0.1573	0.0147
	HYBRID	1.2228	1.5990	0.4006
	MPSD	8.6098	9.8166	4.7123
	RMSE	0.1308	0.1448	0.0689
	MSE	0.0171	0.0209	0.0047
Dubinin–Radushkevich	q_D (mg/g)	4.7958	5.1317	6.500
	K_D	0.0002	0.0001	2×10^{-8}
	R^2	0.9343	0.9365	0.9485
	χ^2	0.6385	0.4445	0.2709
	SSE	0.9925	0.9777	0.8196
	G^2	1.2288	0.9384	–0.1488
	HYBRID	6.1783	5.3951	3.9163
	MPSD	21.755	18.205	14.318
	RMSE	0.3321	0.3296	0.3020
	MSE	0.1103	0.1086	0.0911

Table 7
Adsorption capacity of Crystal violet dye with various adsorbents

Adsorbent	Adsorption capacity (mg/g)	Isotherm	Reference
Neem sawdust	4.44	Langmuir	[99]
Sagaun sawdust	3.50	Langmuir	[100]
Sugarcane dust	3.80	Langmuir	[101]
Tamarind seed powder	3.50×10^{-5} mol/g	Freundlich	[102]
Soil silver nanoparticle	1.92	Langmuir	[103]
Magnetic zeolite	0.97	Langmuir	[104]
Bottom ash	0.90 mol/g	Freundlich	[53]
Groundnut shell	0.524	Freundlich	[105]
Bean pod	0.38	Freundlich	[105]
Fly ash	9.76×10^{-5} mol/g	Freundlich	[106]
Coal fly ash	4E-05 mol/g	Langmuir	[107]
Sewage sludge	3.87	Freundlich	This study

3.5. Thermodynamic parameters

The data obtained from the adsorption isotherms were used to calculate thermodynamic parameters. Table 9 shows the change in standard free energy ($\Delta G°$), enthalpy ($\Delta H°$), and entropy ($\Delta S°$) of adsorption for Crystal violet dye computed using standard methods [Eqs. (12) and (13)]. The process's viability and the spontaneous nature of adsorption were shown by the negative free energy value (–0.3693 kJ/mol). The presence of a positive enthalpy value (0.2572 kJ/mol) suggested that the process was endothermic. The similar results were shown in literature [107]. The positive value of $\Delta S°$ (0.0021 kJ/mol·K) showed the increased randomness at the solid-solution interface due to the affinity of the adsorbent for the dye.

4. Conclusion

On the basis of results, it can be concluded that the activated sewage sludge exhibited ability for the adsorption of dyes from aqueous solution. The pH played an important role in adsorption of Crystal violet dye. The adsorption capacity of Crystal violet dye was 9.508 mg/g at an adsorbent dosage of 10 g/L, pH 5.0 and temperature 30°C. The contact time was found to be 180 min. Freundlich model was found to have the highest regression (0.9898) and lowest chi-square values (0.0761) and hence fitted well. The fitness of Freundlich model indicated the formation of multilayer of the adsorbate on the outer surface of sewage sludge. Kinetic studies showed that the adsorption of Crystal violet dye followed pseudo-second-order kinetics as supported by R^2 value (0.9999) and lowest error function value ($\chi^2 = 0.0004$). Thermodynamic parameters showed that adsorption of Crystal violet dye was spontaneous and endothermic under experimental conditions. The cost of developed activated sludge was very nominal (approx. INR 5/kg) since sewage sludge is available free of cost. Hence, industries which are producing dye-containing effluents may be benefitted from the applicability of activated sludge as dye removal strategy.

Authors are grateful to Dr. A.K. Sinha, Dr. M. K. Tiwari, and Dr. Rashmi Singh (RRCAT Indore) for providing the facility to carry out the characterization of samples.

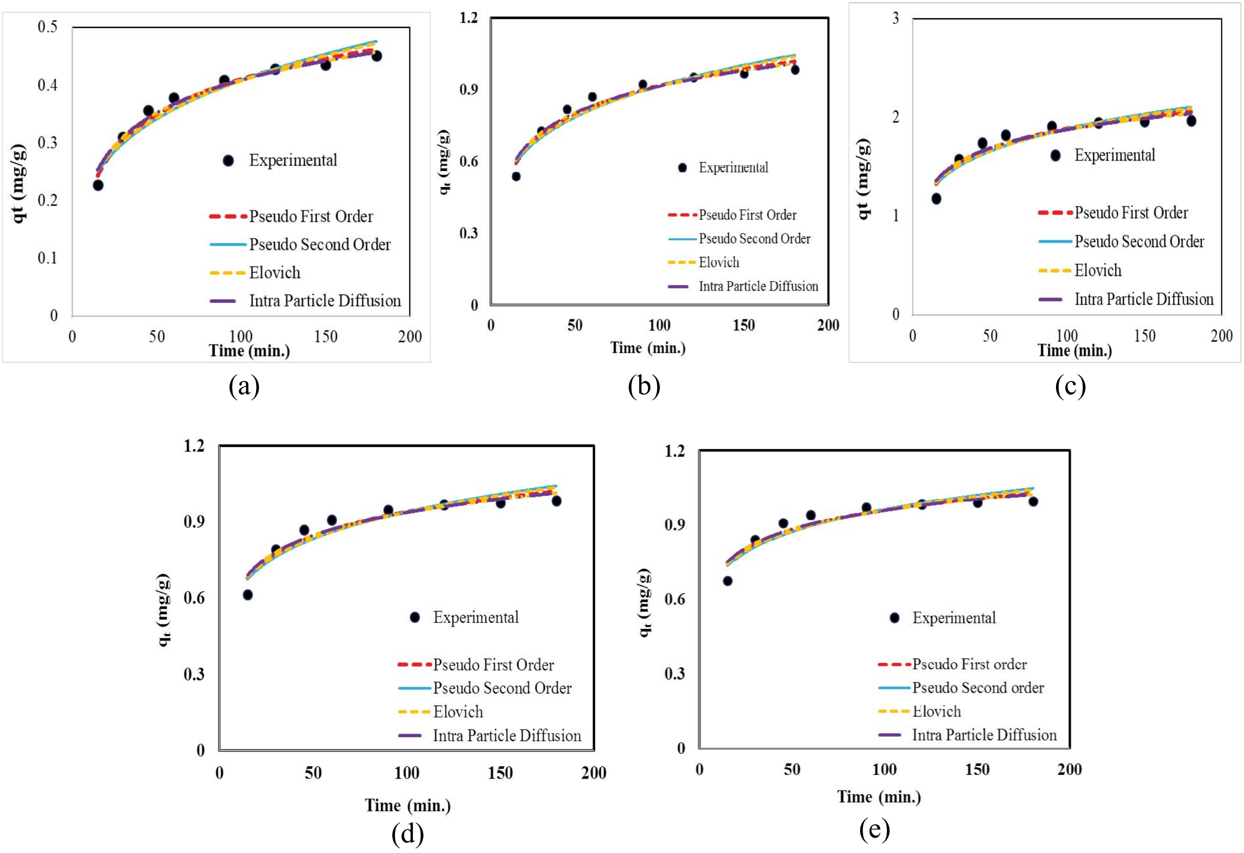

(a) (b) (c)

(d) (e)

Fig. 9. Predicted curve fits for the kinetics of Crystal violet dye adsorption onto sewage sludge at 30°C (a) 5 ppm, (b) 10 ppm, (c) 20 ppm, (d) 40°C and (e) 50°C.

Table 8
Parameters and error function data for kinetic models studied for the sorption of Crystal violet dye onto activated sewage sludge

Isotherm model	Parameters	30°C			40°C (10 ppm)	50°C (10 ppm)
		5 ppm	10 ppm	20 ppm		
Pseudo-first-order	K_{ad}	0.0429	0.0495	0.0583	0.0617	0.9734
	q_e (mg/g)	0.4298	0.9486	1.9315	0.9586	0.0728
	R^2	0.9891	0.9774	0.9867	0.9777	0.9793
	χ^2	0.0032	0.0072	0.0070	0.0054	0.0040
	SSE	0.0016	0.0052	0.0110	0.0042	0.0034
	G^2	0.0224	0.0332	0.0369	0.0222	0.0149
	HYBRID	0.0631	0.1168	0.1155	0.0881	0.0672
	MPSD	3.2971	4.1022	2.7666	3.3865	2.8383
	RMSE	0.0122	0.0255	0.0370	0.0229	0.0207
	MSE	0.0001	0.0006	0.0014	0.0005	0.0004
Pseudo-second-order	K_2	0.1182	1.0629	0.0427	0.0942	0.1212
	q_e (mg/g)	0.4894	0.0669	2.1268	1.0504	1.0511
	R^2	0.9992	0.9985	0.9924	0.9967	0.9951
	χ^2	0.0001	0.0004	0.0040	0.0007	0.0009
	SSE	4.3E-05	0.0003	0.0062	0.0006	0.0008
	G^2	6.4E-05	–0.0025	–0.0055	–0.0018	–0.0011
	HYBRID	0.0017	0.0078	0.0670	0.0130	0.0159
	MPSD	0.6358	1.0817	2.1291	1.3023	1.3933
	RMSE	0.0023	0.0065	0.0279	0.0088	0.0100
	MSE	5.4E-06	0.0086	0.0008	0.0001	0.0001

(Continued)

Table 8

Isotherm model	Parameters	30°C			40°C (10 ppm)	50°C (10 ppm)
		5 ppm	10 ppm	20 ppm		
Intraparticle diffusion	K_{int} (mg/g·min$^{0.5}$)	0.0211	0.0412	0.0707	0.0335	0.0282
	C_i (L/mg)	0.1895	0.4858	1.1459	0.5894	0.6661
	R^2	0.9188	0.8918	0.8557	0.8766	0.8758
	χ^2	0.0135	0.0335	0.0745	0.0292	0.0245
	SSE	0.0044	0.0249	0.1186	0.0233	0.0206
	G^2	0.0139	0.0344	0.0766	0.0298	0.0250
	HYBRID	0.2457	0.0609	1.3577	0.5232	0.4354
	MPSD	9.4726	9.7494	9.8947	8.5578	7.5295
	RMSE	0.0233	0.0558	0.1218	0.0540	0.0508
	MSE	0.0005	0.0031	0.0148	0.0029	0.0025
Elovich kinetics	α (mg/g)	0.0975	0.3575	1.6109	1.0888	3.5597
	β (g/mg)	11.488	5.8116	3.3245	7.0547	8.2915
	R^2	0.9804	0.9636	0.9360	0.9487	0.9422
	χ^2	0.0038	0.0112	0.0330	0.0121	0.0114
	SSE	0.0018	0.0084	0.0526	0.0097	0.0096
	G^2	0.0233	0.0113	0.0333	0.0122	0.0114
	HYBRID	0.0854	0.1933	0.5722	0.2077	0.1952
	MPSD	4.3573	5.3396	6.2640	5.2709	4.9488
	RMSE	0.0134	0.0324	0.0811	0.0348	0.0346
	MSE	0.0001	0.0084	0.0065	0.0012	0.0012

Table 9
Thermodynamic parameters for the uptake of Crystal violet dye onto activated sewage sludge

Temperature	–ΔG° (kJ/mol)	ΔH° (kJ/mol)	ΔS° (kJ/mol·K)
30°C	0.3693	0.2572	0.0021
40°C	0.3900	59.263	0.1906
50°C	2.2958		

References

[1] T. Adane, A.T. Adugna, E. Alemayehu, Textile industry effluent treatment techniques, J. Chem., 2021 (2021) 1–14, doi: 10.1155/2021/5314404.

[2] C.R. Holkar, A.J. Jadhav, D.V. Pinjari, N.M. Mahamuni, A.B. Pandit, A critical review on textile wastewater treatments: possible approaches, J. Environ. Manage., 182 (2016) 351–366.

[3] R.V. Kandisa, K.N. Saibaba, K.B. Shaik, R. Gopinath, Dye removal by adsorption: a review, J. Biorem. Biodegrad., 7 (2016) 371, doi: 10.4172/2155-6199.1000371.

[4] Z. Wang, M. Xue, K. Huang, Z. Liu, Textile Dyeing Wastewater Treatment, P.J. Hauser, Ed., Advances in Treating Textile Effluent, InTechOpen, 2011, pp. 91–116, doi: 10.5772/22670.

[5] P. Bhatt, A. Rani, Textile dyeing and printing industry: an environmental hazard, Asian Dyer, 10 (2013) 51–54.

[6] J. Wang, Z. Bai, Fe-Based catalysts for heterogeneous catalytic ozonation of emerging contaminants in water and wastewater, Chem. Eng. J., 312 (2017) 79–98.

[7] C. Zaharia, M.R. Tudora, I.C. Stancu, B. Galateanu, A. Lungu, C. Cincu, Characterization and deposition behaviour of silk hydrogels soaked in simulated body fluid, Mater. Sci. Eng., 32 (2012) 945–952.

[8] V.K. Gupta, Suhas, Application of low-cost adsorbents for dye removal-a review, J. Environ. Manage., 90 (2009) 2313–2342.

[9] W. Konicki, D. Sibera, E. Mijoska, Z. Lendzion-Bieluń, U. Narkiewicz, Equilibrium and kinetic studies on acid dye Acid Red 88 adsorption by magnetic $ZnFe_2O_4$ spinel ferrite nanoparticles, J. Colloid Interface Sci., 398 (2013) 152–160.

[10] B. Lellis, C.Z. Fávaro-Polonio, J.A. Pamphile, J.C. Polonio, Effects of textile dyes on health and the environment and bioremediation potential of living organisms, Biotechnol. Res. Innovation, 3 (2019) 275–290.

[11] U.B. Deshannavar, G.M. Ratnamala, P.B. Kalburgi, M. El-Harbawi, A. Agarwal, M. Shet, M. Teli, P. Bhandare, Optimization, kinetic and equilibrium studies of disperse yellow 22 dye removal from aqueous solutions using Malaysian teak wood sawdust as adsorbent, Indian Chem. Eng., 58 (2016) 12–28.

[12] A. Nasar, S. Shakoor, Remediation of Dyes from Industrial Wastewater Using Low-Cost Adsorbents, Inamuddin, A. Al-Ahmed, Eds., Applications of Adsorption and Ion Exchange Chromatography in Wastewater Treatment, Materials Research Foundations, Millersville PA, USA, 2017, pp. 1–33, doi: 10.21741/9781945291333-1.

[13] S. Senthil Kumar, P. Kalaamani, C.V. Subburaam, Liquid-phase adsorption of Crystal violet onto activated carbons derived from male flowers of a coconut tree, J. Hazard. Mater., 136 (2006) 800–808.

[14] H. He, S. Yang, K. Yu, Y. Ju, C. Sun, L. Wang, Microwave induced catalytic degradation of Crystal violet in nano-nickel dioxide suspensions, J. Hazard. Mater., 173 (2010) 393–400.

[15] S. Mani, R.N. Bhargava, Exposure to Crystal violet, its toxic, genotoxic, and carcinogenic effects on the environment and its degradation and detoxification for environmental safety, Rev. Environ. Contam. Toxicol., 237 (2016) 71–104.

[16] X. Pang, L. Sellaoui, D. Franco, M.S. Netto, J. Georgin, G.L. Dotto, M.K.A Shayeb, H. Belmabrouk, A. Bonilla-Petriciolet, Z. Li, Preparation and characterization of a novel mountain soursop seeds powder adsorbent and its application for the removal of Crystal violet and methylene blue from aqueous solutions, Chem. Eng. J., 391 (2020) 123617, doi: 10.1016/j.cej.2019.123617.

[17] M. Otero, F. Rozada, L.F. Calvo, A.I. García, A. Morán, Elimination of organic water pollutants using adsorbents obtained from sewage sludge, Dyes Pigm., 57 (2003) 55–65.

[18] Q. Zhang, T. Zhang, T. He, L. Chen, Removal of Crystal violet by clay/PNIPAm nanocomposite hydrogels with various clay contents, Appl. Clay Sci., 90 (2014) 1–5.

[19] M.R. Gadekar, M.M. Ahammed, Coagulation/flocculation process for dye removal using water treatment residuals: modelling through artificial neural networks, Desal. Water Treat., 57 (2016) 26392–26400.

[20] A. Ikhlaq, M. Kazim, F. Javed, K.S. Joya, F. Anwar, Combined catalytic ozonation and electro flocculation process for the removal of basic yellow 28 in wastewater, Desal. Water Treat., 127 (2018) 354–363.

[21] S. Mishra, P. Chowdhary, R.N. Bharagava, Chapter 1 – Conventional Methods for the Removal of Industrial Pollutants, Their Merits and Demerits, R.N. Bharagava, P. Chowdhary, Eds., Emerging and Eco-Friendly Approaches for Waste Management, Springer Nature Singapore Pte Ltd., Singapore, 2019, pp. 1–31.

[22] M.C. Collivignarelli, A. Abbà, M.C. Miino, S. Damiani, Treatments for colour removal from wastewater: state of the art, J. Environ. Manage., 236 (2019) 727–745.

[23] A. Ikhlaq, T. Aslam, A.M. Zafar, F. Javed, H.M.S. Munir, Combined ozonation and adsorption system for the removal of heavy metals from municipal wastewater: effect of COD removal, Desal. Water Treat., 159 (2019) 304–309.

[24] A. Ikhlaq, F. Javed, M.S. Munir, S. Hussain, K.S. Joya, A.M. Zafar, Application of heterogeneous iron loaded zeolite A catalyst in photo-Fenton process for the removal of safranin in wastewater, Desal. Water Treat., 148 (2019) 152–161.

[25] A. Ikhlaq, H.M.S. Munir, A. Khan, F. Javed, K.S. Joya, Comparative study of catalytic ozonation and Fenton-like processes using iron-loaded rice husk ash as catalyst for the removal of methylene blue in wastewater, Ozone Sci. Eng., 41 (2019) 250–260.

[26] H.S. Munir, F. Nadeem, I. Amir, K. Mohsin, J. Farhan, M. Hina, Removal of colour and COD from paper and pulp industry wastewater by ozone and combined ozone/UV process, Desal. Water Treat., 137 (2019) 154–161.

[27] F. Javed, N. Feroze, N. Ramzan, A. Ikhlaq, M. Kazmi, H.M.S. Munir, Treatment of Reactive Red 241 dye by electro coagulation/biosorption coupled process in a new hybrid reactor, Desal. Water Treat., 166 (2019) 83–91.

[28] N. Noreena, M. Kazmib, N. Ferozea, F. Javedd, H. Ghulam, H.M.S.M. Qutabd, Treatment of methylene blue in aqueous solution by electrocoagulation/micro-crystalline cellulosic adsorption combined process, Desal. Water Treat., 203 (2020) 379–387.

[29] F. Deniz, R. Aysun Kepekci, Dye biosorption onto pistachio by-product: a green environmental engineering approach, J. Mol. Liq., 219 (2016) 194–200.

[30] I. Anastopoulos, I. Pashalidis, A.G. Orfanos, I.D. Manariotis, T. Tatarchuk, L. Sellaoui, A. Bonilla-Petriciolet, A. Mittal, A. Núñez-Delgado, Removal of caffeine, nicotine and amoxicillin from (waste)waters by various adsorbents. A review, J. Environ. Manage., 261 (2020) 110236, doi: 10.1016/j.jenvman.2020.110236.

[31] A. Mittal, R. Ahmad, I. Hasan, Poly(methyl methacrylate)-grafted alginate/Fe_3O_4 nanocomposite: synthesis and its application for the removal of heavy metal ions, Desal. Water Treat., 57 (2016) 19820–19833.

[32] A. Mittal, R. Ahmad, I. Hasan, Iron oxide-impregnated dextrin nanocomposite: synthesis and its application for the biosorption of Cr(VI) ions from aqueous solution, Desal. Water Treat., 57 (2016) 15133–15145.

[33] N. Ariffin, M.M.A.B. Abdullah, M.R.R.M.A. Zainol, M.F. Murshed, M.A. Faris, R. Bayuaji, Review on adsorption of heavy metal in wastewater by using geopolymer, MATEC Web Conf., 97 (2017) 01023, doi: 10.1051/matecconf/20179701023.

[34] N. Sivarajasekar, R. Baskar, Agriculture waste biomass valorisation for cationic dyes sequestration: a concise review, J. Chem. Pharm. Res., 7 (2015) 737–748.

[35] S. Dawood, T. Sen, Review on dye removal from its aqueous solution into alternative cost effective and non-conventional adsorbents, J. Chem. Proc. Eng., 1 (2014) 1–11.

[36] M.A.M. Salleh, D.K. Mahmoud, W.A.W.A. Karim, A. Idris, Cationic and anionic dye adsorption by agricultural solid wastes: a comprehensive review, Desalination, 280 (2011) 1–13.

[37] M.A. Oturan, J.J. Aaron, Advanced oxidation processes in water/wastewater treatment: principles and applications. A review, Crit. Rev. Env. Sci. Technol., 44 (2014) 2577–2641.

[38] M. Brienza, I.A. Katsoyiannis, Sulfate radical technologies as tertiary treatment for the removal of emerging contaminants from wastewater, Sustainability, 9 (2017) 1604, doi: 10.3390/su9091604.

[39] E.M. Cuerda-Correa, M.F. Alexandre-Franco, C. Fernández-González, Advanced oxidation processes for the removal of antibiotics from water. An overview, Water, 12 (2020) 102, doi: 10.3390/w12010102.

[40] H.M.S. Munir, N. Feroze, N. Ramzan, M. Sagir, M. Babar, M.S. Tahir, J. Shamshad, M. Mubashir, K.S. Khoo, Fe-zeolite catalyst for ozonation of pulp and paper wastewater for sustainable water resources, Chemosphere, 297 (2022) 134031, doi: 10.1016/j.chemosphere.2022.134031.

[41] A. Ikhlaq, F. Javed, A. Niaz, H.M.S. Munir, F. Qi, Combined UV catalytic ozonation process on iron loaded peanut shell ash for the removal of methylene blue from aqueous solution, Desal. Water Treat., 200 (2020) 231–240.

[42] S. Nazir, A. Ikhlaq, F. Javed, Z. Asif, H.M.S. Munir, S. Sajjad, Catalytic ozonation on iron-loaded rice husk ash/peanut shell ash for the removal of erythromycin in water, Environ. Eng. Manage. J., 19 (2020) 829–837.

[43] S.P. Druzian, N.P. Zanatta, R.K. Borchardt, L.N. Côrtes, A.F. Streit, E.C. Severo, J.O. Gonçalves, E.L. Foletto, E.C. Lima, G.L. Dotto, Chitin-psyllium based aerogel for the efficient removal of Crystal violet from aqueous solutions, Int. J. Biol. Macromol., 15 (2021) 366–376.

[44] D.O. Omokpariola, Experimental modelling Studies on the removal of Crystal violet, methylene blue and malachite green dyes using *Theobroma cocoa* (Cocoa Pod Powder), J. Chem. Lett., 2 (2021) 9–24.

[45] Y.H. Wu, K. Xue, Q.L. Ma, T. Ma, Y.L. Ma, Y.G. Sun, W.X. Ji, Removal of hazardous Crystal violet dye by low-cost P-type zeolite/carbon composite obtained from in situ conversion of coal gasification fine slag, Microporous Mesoporous Mater., 312 (2021) 110742, doi: 10.1016/j.micromeso.2020.110742.

[46] K.M. Elsherif, A. El-Dali, A.A. Alkarewi, A.M. Ewlad-Ahmed, A. Treban, Adsorption of Crystal violet dye onto olive leaves powder: equilibrium and kinetic studies, Chem. Int., 7 (2021) 79–89.

[47] R. Ahmad, Studies on adsorption of Crystal violet dye from aqueous solution onto coniferous pinus bark powder (CPBP), J. Hazard. Mater., 171 (2009) 767–773.

[48] K. Mohanty, J.T. Naidu, B.C. Meikap, M.N. Biswas, Removal of Crystal violet from wastewater by activated carbons prepared from rice husk, Ind. Eng. Chem. Res., 45 (2006) 5165–5171.

[49] M. Alshabanat, G. Alsenani, R. Almufarij, Removal of Crystal violet dye from aqueous solutions onto date palm fiber by adsorption technique, J. Chem., 2013 (2013) 1–6.

[50] H.J. Kumari, P. Krishnamoorthy, T.K. Arumugam, S. Radhakrishnan, D. Vasudevan, An efficient removal of Crystal violet dye from waste water by adsorption onto TLAC/Chitosan composite: a novel low-cost adsorbent, Int. J. Biol. Macromol., 96 (2017) 324–333.

[51] S. Chakraborty, A. Mukherjee, S. Das, N.R. Maddela, S. Iram, P. Das, Study on isotherm, kinetics, and thermodynamics of adsorption of Crystal violet dye by calcium oxide modified fly ash, Environ. Eng. Res., 26 (2021) 190372, doi: 10.4491/eer.2019.372.

[52] S. Sultana, K. Islam, M.A. Hasan, H.M. Jawad Khan, M. Azizur R. Khan, A. Deb, Md. Al Raihan, M.W. Rahman, Adsorption of Crystal violet dye by coconut husk powder: isotherm, kinetics and thermodynamics perspectives, Environ. Nanotechnol. Monit. Manage., 17 (2022) 100651, doi: 10.1016/j.enmm.2022.100651.

[53] A. Mittal, J. Mittal, A. Malviya, D. Kaur, V.K. Gupta, Adsorption of hazardous dye Crystal violet from wastewater by waste materials, J. Colloid Interface Sci., 343 (2010) 463–473.

[54] A. Saeed, M. Sharif, M., M. Iqbal, Application potential of grapefruit peel as dye sorbent: kinetics, equilibrium and mechanism of Crystal violet adsorption, J. Hazard. Mater., 179 (2010) 564–572.

[55] T.A. Khan, R. Rahman, E.A. Khan, Decolorization of bismarck brown R and Crystal violet in liquid phase using modified pea peels: non-linear isotherm and kinetics modelling, Model. Earth Syst. Environ., 2 (2016) 1–11.

[56] Z. Liu, T.A. Khan, M.A. Islam, U. Tabrez, A review on the treatment of dyes in printing and dyeing wastewater by plant biomass carbon, Bioresour. Technol., 354 (2022) 127168, doi: 10.1016/j.biortech.2022.127168.

[57] CPCB, Inventorization of Sewage Treatment Plants, Control of Urban Pollution Series: CUPS/84/2015-16 (Accessed on 18 March 2015).

[58] M. Khwairakpam, R. Bhargava, Vermitechnology for sewage sludge recycling, J. Hazard. Mater., 161 (2009) 948–954.

[59] R.K. Sinha, S. Herat, G. Bharambe, A. Brahambhatt, Vermistabilization of sewage sludge (biosolids) by earthworms: converting a potential biohazard destined for landfill disposal into a pathogen-free, nutritive and safe biofertilizer for farms, Waste Manage. Res., 28 (2010) 872–881.

[60] J. Wang, J. Wang, Application of radiation technology to sewage sludge processing: a review, J. Hazard. Mater., 143 (2007) 2–7.

[61] M. Jaeger, M. Mayer, The Noell Conversion Process – a gasification process for the pollutant-free disposal of sewage sludge and the recovery of energy and materials, Water Sci. Technol., 41 (2000) 37–44.

[62] A.N. Ghiocel, V.N. Panaitescu, Using sewage sludge as an alternative fuel for the cement production process, IOP Conf. Ser.: Mater. Sci. Eng., 400 (2018) 022029.

[63] I.C. Pereira, K.Q. Carvalho, F.H. Passig, R.C. Ferreira, R.C.P. Rizzo-Domingues, M.I. Hoppen, G. Macioski, A. Nagalli, F. Perretto, Thermal and thermal-acid treated sewage sludge for the removal of dye Reactive Red 120: characteristics, kinetics, isotherms, thermodynamics and response surface methodology design, J. Environ. Chem. Eng., 6 (2018) 7233–7246.

[64] C. Jindarom, V. Meeyoo, B. Kitiyanan, T. Rirksomboon, P. Rangsunvigit, Surface characterization and dye adsorptive capacities of char obtained from pyrolysis/gasification of sewage sludge, Chem. Eng. J., 133 (2007) 239–246.

[65] F. Rozada, L.F. Calvo, A.I. Garcıa, J. Martın-Villacorta, M. Otero, Dye adsorption by sewage sludge-based activated carbons in batch and fixed-bed systems, Bioresour. Technol., 87 (2003) 221–230.

[66] Y. Tang, Q. Zhou, Y. Zeng, Y. Peng, Bio-adsorption of dyes from aqueous solution by powdered excess sludge (PES): kinetic, isotherm, and thermodynamic study, J. Dispersion Sci. Technol., 38 (2017) 347–354.

[67] A. Valério Filho, R. Xavaré Kulman, L. Vaz Tholozan, A.R. Felkl de Almeida, G. Silveira da Rosa, Preparation and characterization of activated carbon obtained from water treatment plant sludge for removal of cationic dye from wastewater, Processes, 8 (2020) 1549, doi: 10.3390/pr8121549.

[68] P. Shrivastava, M.K. Dwivedi, V. Malviya, P. Jain, Process development for the removal of Malachite green dye from wastewater using sewage sludge (STP) as an adsorbent, AIP Conf. Proc., 2369 (2021) 020218.

[69] H.M.F. Freundlich, Over the adsorption in solution, J. Phys. Chem., 57 (1906) 1100–1107.

[70] I. Langmuir, The constitution and fundamental properties of solids and liquids. Part I. Solids, J. Am. Chem. Soc., 38 (1916) 2221–2295.

[71] O.J.D.L. Redlich, D.L. Peterson, A useful adsorption isotherm, J. Phys. Chem., 63 (1959) 1024–1024.

[72] M.M. Dubinin, The equation of the characteristic curve of activated charcoal, In Dokl. Akad. Nauk. SSSR., 55 (1947) 327–329.

[73] S.K. Lagergren, About the theory of so-called adsorption of soluble substances, Sven. Vetenskapsakad. Handingarl., 24 (1898) 1–39.

[74] Y.S. Ho, G. McKay, The kinetics of sorption of basic dyes from aqueous solution by sphagnum moss peat, Can. J. Chem. Eng., 76 (1998) 822–827.

[75] T.A. Khan, S. Dahiya, E.A. Khan, Removal of direct red 81 from aqueous solution by adsorption onto magnesium oxide-coated kaolinite: isotherm, dynamics and thermodynamic studies, Environ. Prog. Sustainable Energy, 36 (2017) 45–58.

[76] M.F. Siddiqui, E.A. Khan, T. Alam Khan, Synthesis of MoO_3/poly pyrrole nanocomposite and its adsorptive properties toward cadmium(II) and nile blue from aqueous solution: equilibrium isotherm and kinetics modelling, Environ. Prog. Sustainable Energy, 38 (2019) e13249.

[77] Y.S. Ho, G. McKay, Comparative sorption kinetic studies of dye and aromatic compounds onto fly ash, J. Environ. Sci. Health. Part A Toxic/Hazard. Subst. Environ. Eng., 34 (1999) 1179–1204.

[78] Y.C. Wong, Y.S. Szeto, W. Cheung, G. McKay, Adsorption of acid dyes on chitosan—equilibrium isotherm analyses, Process Biochem., 39 (2004) 695–704.

[79] A. Malek, S. Farooq, Comparison of isotherm models for hydrocarbon adsorption on activated carbon, AIChE J., 42 (1996) 3191–3201.

[80] A.R. Khan, I.R. Al-Waheab, A. Al-Haddad, A generalized equation for adsorption isotherms for multi-component organic pollutants in dilute aqueous solution, Environ. Technol., 17 (1996) 13–23.

[81] T.A. Khan, E.A. Khan, Removal of basic dyes from aqueous solution by adsorption onto binary iron-manganese oxide coated kaolinite: non-linear isotherm and kinetics modeling, Appl. Clay Sci., 107 (2015) 70–77.

[82] T.A. Khan, M. Nouman, D. Dua, S.A. Khan, S.S. Alharthi, Adsorptive scavenging of cationic dyes from aquatic phase by H_3PO_4 activated Indian jujube (*Ziziphus mauritiana*) seeds based activated carbon: isotherm, kinetics, and thermodynamic study, J. Saudi Chem. Soc., 26 (2022) 101417.

[83] Y.S. Ho, J.F. Porter, G. McKay, Equilibrium isotherm studies for the sorption of divalent metal ions onto peat: copper, nickel and lead single component systems, Water Air Soil Pollut., 141 (2002) 1–33.

[84] Y.S. Ho, Selection of optimum sorption isotherm, Carbon, 42 (2004) 2115–2116.

[85] O.T. Hanna, O.C. Sandall, Computational Methods in Chemical Engineering, Prentice Hall, New Jersey, 1995. Available at: https://doi.org/10.21741/9781945291333-1

[86] J.C.Y. Ng, W.H. Cheung, G. McKay, Equilibrium studies of the sorption of Cu(II) ions onto chitosan, J. Colloid Interface Sci., 255 (2002) 64–74.

[87] H. Chernoff, E.L. Lehmann, The Use of Maximum Likelihood Estimates in χ^2 Tests for Goodness of Fit, In Selected Works of EL Lehmann, Springer, Boston, MA, 2012, pp. 541–549, doi: 10.1007/978-1-4614-1412-4_47.

[88] S.J. Allen, Q. Gan, R. Matthews, P.A. Johnson, Comparison of optimized isotherm models for basic dye adsorption by kudzu, Bioresour. Technol., 88 (2003) 143–152.

[89] D.W. Marquardt, An algorithm for least-squares estimation of nonlinear parameters, J. Soc. Ind. Appl. Math., 11 (1963) 431–441.

[90] S.C. Tsai, K.W. Juang, Comparison of linear and nonlinear forms of isotherm models for strontium sorption on a sodium bentonite, J. Radioanal. Nucl. Chem., 243 (2000) 741–746.

[91] W.A.H. Altowayti, N. Othman, A. Al-Gheethi, M. Dzahir, S.M. Asharuddin, A.F. Alshalif, I.M. Nasser, H.A. Tajarudin, F.A.H. Al-Towayti, Adsorption of Zn^{2+} from synthetic wastewater using dried watermelon rind (D-WMR): an overview of nonlinear and linear regression and error analysis, Molecules, 26 (2021) 6176.

[92] P. Shrivastava, V. Malviya, M.K. Dwivedi, M.K. Tiwari, Elemental investigation of sewage sludge samples using synchrotron radiation based XRF spectrometry, Dickensian J., 22 (2022) 777–785.

[93] EPA, Land Application of Sewage Sludge, Environmental Protection Agency, Part 503. Standards for the Use or Disposal of Sewage Sludge (Section 503.13), Pollutant Limits, United States Office of Enforcement, Environmental and Compliance

Assurance, Protection Agency Washington, DC 20460, 1994.

[94] N. Gao, J. Li, B. Qi, A. Li, Y. Duan, Z. Wang, Thermal analysis and products distribution of dried sewage sludge pyrolysis, J. Anal. Appl. Pyrolysis, 105 (2014) 43–48.

[95] M. Kowalski, K. Kowalska, J. Wiszniowski, J. Turek-Szytow, Qualitative analysis of activated sludge using FT-IR technique, Chem. Pap., 72 (2018) 2699–2706.

[96] A. Goksu, M.K. Tanaydin, Adsorption of hazardous Crystal violet dye by almond shells and determination of optimum process conditions by Taguchi method, Desal. Water Treat., 88 (2017) 189–199.

[97] S.C. Pan, C.C. Lin, D.H. Tseng, Reusing sewage sludge ash as adsorbent for copper removal from wastewater, Resour. Conserv. Recycl., 39 (2003) 79–90.

[98] P.S. Kumar, S. Ramalingam, C. Senthamarai, M. Niranjanaa, P. Vijayalakshmi, S. Sivanesan, Adsorption of dye from aqueous solution by cashew nut shell: studies on equilibrium isotherm, kinetics and thermodynamics of interactions, Desalination, 261 (2010) 52–60.

[99] N. Laskar, U. Kumar, Adsorption of Crystal violet from wastewater by modified bambusa tulda, KSCE J. Civ. Eng., 22 (2018) 2755–2763.

[100] S.D. Khattri, M.K. Singh, Colour removal from synthetic dye wastewater using a bioadsorbent, Water Air Soil Pollut., 120 (2000) 283–294.

[101] S. Khattri, M. Singh, Use of Sagaun sawdust as an adsorbent for the removal of Crystal violet dye from simulated wastewater, Environ. Prog. Sustainable Energy, 31 (2012) 435–442.

[102] S.D. Khattri, M.K. Singh, Colour removal from dye wastewater using sugar cane dust as an adsorbent, Adsorpt. Sci. Technol., 17 (1999) 269–282.

[103] H. Patel, R.T. Vashi, Adsorption of Crystal violet dye onto tamarind seed powder, E-J. Chem., 7 (2010) 975–984.

[104] M.K. Satapathy, P. Das, Optimization of Crystal violet dye removal using novel soil-silver nanocomposite as nanoadsorbent using response surface methodology, J. Environ. Chem. Eng., 2 (2014) 708–714.

[105] O.S. Amodu, T.V. Ojumu, S.K. Ntwampe, O.S. Ayanda, Rapid adsorption of Crystal violet onto magnetic zeolite synthesized from fly ash and magnetite nanoparticles, J. Encapsulation Adsorpt. Sci., 5 (2015) 191–203.

[106] L.K. Akinola, A.M. Umar, Adsorption of Crystal violet onto adsorbents derived from agricultural wastes: kinetic and equilibrium studies, J. Appl. Sci. Environ. Manage., 19 (2015) 279–288.

[107] D. Mohan, K.P. Singh G. Singh, K. Kumar, Removal of dyes from wastewater using fly ash, a low-cost adsorbent, Ind. Eng. Chem. Res., 41 (2002) 3688–3695.

[108] L. Li, S. Wang, Z. Zhu, Geopolymeric adsorbents from fly ash for dye removal from aqueous solution, J. Colloid Interface Sci., 300 (2006) 52–59.

[109] X.L. Gong, H.Q. Lu, K. Li, W. Li, Effective adsorption of Crystal violet dye on sugarcane bagasse–bentonite/sodium alginate composite aerogel: Characterisation, experiments, and advanced modelling, Sep. Purif. Technol., 286 (2022) 120478, doi: 10.1016/j.seppur.2022.120478.